2014 AMOS Technical Conference, 9-12 September, 2014, Maui, Hawaii, USA

Improved Space Object Orbit Determination Using CMOS Detectors

J. Silha[1,2]
[1] Astronomical Institute, University of Bern, CH-3012 Bern, Switzerland,
[2]Faculty of Mathematics, Physics and Informatics, Comenius University, Mlynská dolina, 84248 Bratislava, Slovakia

T. Schildknecht
Astronomical Institute, University of Bern, CH-3012 Bern, Switzerland
T. Flohrer
Space Debris Office, ESA/ESOC, Germany

Abstract

CMOS-sensors, or in general Active Pixel Sensors (APS), are rapidly replacing CCDs in the consumer camera market. Due to significant technological advances during the past years these devices start to compete with CCDs also for demanding scientific imaging applications, in particular in the astronomy community. CMOS detectors offer a series of inherent advantages compared to CCDs, due to the structure of their basic pixel cells, which each contains their own amplifier and readout electronics. The most prominent advantages for space object observations are the extremely fast and flexible readout capabilities, feasibility for electronic shuttering and precise epoch registration, and the potential to perform image processing operations on-chip and in real-time.
Here, the major challenges and design drivers for ground-based and space-based optical observation strategies for objects in Earth orbit have been analyzed. CMOS detector characteristics were critically evaluated and compared with the established CCD technology, especially with respect to the above mentioned observations.
Finally, we simulated several observation scenarios for ground- and space-based sensor by assuming different observation and sensor properties. We will introduce the analyzed end-to-end simulations of the ground- and space-based strategies in order to investigate the orbit determination accuracy and its sensitivity which may result from different values for the frame-rate, pixel scale, astrometric and epoch registration accuracies. Two cases were simulated, a survey assuming a ground-based sensor to observe objects in LEO for surveillance applications, and a statistical survey with a space-based sensor orbiting in LEO observing small-size debris in LEO. The ground-based LEO survey uses a dynamical fence close to the Earth shadow a few hours after sunset. For the space-based scenario a sensor in a sun-synchronous LEO orbit, always pointing in the anti-sun direction to achieve optimum illumination conditions for small LEO debris was simulated.

1. INTRODUCTION

This paper introduces and analyzes the end-to-end simulations of ground- and space-based observation strategies for space debris in order to investigate the initial orbit determination accuracy and the sensitivity which mays result from changes in the pixel scale, in the astrometric accuracy, in the epoch registration accuracy and in the exposure time. For ground- and space-based observations of LEO objects high angular velocities and short observations “windows” limit the optical observation possibilities. A large field of view (FOV) with a large detector combined with a fast read-out time is required to acquire tracklets of a sufficient length to enable the orbit determination. Simulated was a ground-based LEO surveillance, where a dynamical fence close to the Earth shadow few hours after the sunset and before the sunrise is discussed. This strategy allows observing LEO objects under the best illumination conditions. In case of a global network of sites, it is possible to implement a leak-proof LEO survey [1]. Also a space-based LEO survey scenario was modeled and will be introduced in this paper. For this type of observation the line of sight (LOS) from a sun-synchronous orbiter is always pointing into the anti-sun direction to achieve the maximum brightness conditions for small LEO particles. The altitude is selected close to the most dense altitude regimes for 1 cm and larger objects. This orbit allows a sensor to cover wide inclination regimes and then increase the coverage for the statistical data. We also investigated the achievable initial orbit determination accuracy for objects in the GEO region using the mentioned LEO observation strategies.

2. ACTIVE PIXEL SENSORS

The so-called Active Pixel Sensors (APS) or Complementary Metal–Oxide–Semiconductor (CMOS) sensors are currently widely used in the commercial consumer area. Due to the more complex technology compared to the Charge-Coupled Device (CCD) sensors, which bring some drawbacks, the CMOS application in the scientific area is still not fully exploited. For the CMOS camera every pixel has its own amplifier, which can be an advantage, as on-chip processing can be applied. On the other hand, this may also have some drawbacks like a pixel to pixel non-uniformity. In general, the quantum efficiencies of CMOS sensors are usually lower than for CCDs. A very huge advantage for CMOS cameras is the possibility to use electronic shutters. Unlike mechanical shutters used with most CCDs, for electronic shutters very high frame-rates can be reached in order of tens to hundreds of frames per second. This capability can be beneficial for the orbit determination and improvement as more observations per object for the same time span can be acquired. Electronic shutters also allow to have very high epoch registration accuracies, which can reach values down to 0.025 ms. For LEO-LEO objects tracking, as we will show later in this paper, this parameter can play an essential role for the initial orbit determination accuracy.
The major interest for us was to determine which parameters can affect the accuracies of initial determined orbits for objects discovered during ground- and space-based surveys, when we use a CMOS instead of a CCD camera. For the astrometry, and consequently the orbit determination accuracy, we chose the following parameters for which the sensitivity analysis was performed:

1. Astrometric accuracy – This parameter is a function of the pixel scale (size of the field of view combined with sensor dimensions), observation conditions, such as atmospheric seeing, and object brightness. Comparable accuracies can be achieved for the CCD, as well for the CMOS.
2. Frame-rate – This parameter is a function of the read-out time. Electronic shutters used for all CMOS cameras can achieve much higher frame-rates than mechanical shutters used by most CCD sensors.
3. Epoch registration accuracy – As we already mentioned, this parameter can be very accurately determined for CMOS sensors, where for the CCD we can expect one to two orders lower accuracy.

Two different observation strategies, which are further introduced in the following section, were investigated: the ground-based surveillance and the space-based survey. For more details about the CMOS sensors properties, their advantages comparing to CCD, and also drawbacks, we refer to [2].

3. OBSERVATION STRATEGIES

For the ground-based LEO surveillance a very complex observation strategies had to be developed. These usually include several sites distributed around the Earth equator, and in the north and south hemisphere. Several telescopes per site are needed, which are creating so-called fences [1, 3]. These sensors should have a very large field of view, or in some cases one large FOV is constructed from few telescopes simultaneously pointing in the adjacent directions. Because of the complexity of LEO surveillance strategies, we assumed in our simulation several simplifications. However, these shouldn't affect considerably the output results concerning initial orbit determination. One of these simplifications is that we assumed only one observation site, namely ESA's Optical Ground Station (OGS) situated at the Teide Observatory, Tenerife, Spain. Our simulated observation strategy was inspired mostly by [1]. In this study the authors are introducing the dynamic fence for LEO surveillance observations. Seven sites are assumed, three placed at the equator and two on the northern and southern hemisphere. There are three telescopes per site with 7°x7° field of view (FOV). Every of these telescopes performed scanning of stripes which cover 14°x49°. This strategy provides a leak-proof survey. FOVs are placed close to the Earth shadow to maximize the illumination for LEO objects. Performing one observation per field (7°x7°) with an exposure of one second and a slew time of two seconds between field, each telescope needs 21 second to cover one stripe of 7°x49°, and 42 seconds to cover the selected region of 14°x49°. According to authors [1] this strategy allows to detect more than 95 % of crossing objects.
In our simulations 14 FOVs close to the Earth shadow were chosen, simulating two telescopes observations. To maximize the total number of crossing objects (objects which crossed the FOV) we chose the FOV equal to 7°x7°. According to [1], one telescope would finish its cycle in 42 seconds resulting in at least two tracklets for objects with angular velocity equal or less than 1000 arc-sec/s. We slightly modified this strategy by assuming only one stripe of 7°x49°, which means one observation per selected FOV every 21 seconds. An example of such a survey is plotted in Fig. 1. Fields marked by pink represent FOVs scanned by the first telescope and fields marked by orange represent FOVs scanned by the second telescope. These fields are always close the earth shadow (gray area). To scan every of these stripes took 21 s, where both stripes are scanned independently.

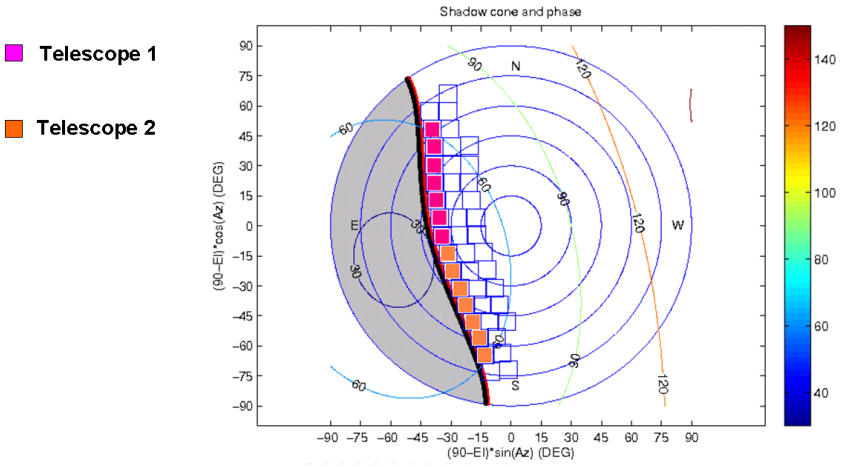

Fig. 1. The sky and the Earth shadow for medium latitude station (lat = 42.5 deg). Local time ~h20 on March 20th. Marked are two stripes, pink and orange for the first and second telescope. Identical stripes were simulated during the ground-based scenario. Figure adapted from [1].

For the space-based sensor simulation, the following parameters were assumed. A sensor, which properties should be suitable for acquiring space-based measurements, an appropriate orbit, which has a great influence on the type, frequency and geometry (position angle, angular velocities) of tracked objects, and an observation strategy, which has to assure that an (initial) orbit could be determined successfully and as accurate as possible.
For choosing the sensor orbit several options can be proposed. The most important task is to decide whether the observations are dedicated to the space debris follow-up observations, or are primarily space debris surveys. Because the advantages of the CMOS sensors are mostly in the increased frame-rates (shorten exposures, fast read out times), increased astrometric accuracy and epoch registration accuracy, their influence would be mostly noticeable during the initial orbit determination of objects with very short arcs. For the space-based sensor (SBS) the tracked LEO objects are usually very close to the sensor, which causes that they are visible only for few seconds and their tracklets consist from only few positions. This can be improved by using higher frame-rates. We decided to have as a primary goal for the simulated space-based scenario a survey of LEO space debris particles and to acquire their statistical orbit distribution that in turn is a relevant input for the development, improvement, and validation of space debris environment models. As a sort of a by-product or secondary aim, also the sensitivity of the initial orbit accuracy for GEO objects to different input parameters was investigated.
The most populated orbital region is near the altitude of 800 km above the Earth surface. By putting the sensor in a region close to this peak on a reasonable orbital inclination, one can widely cover different types of particles in terms of their orbital elements, their distance from sensor, their angular velocity with respect to the sensor and their direction on the image/frame (position angle). To achieve, that even small objects would be detected, the most efficient strategy is to choose that the sensor's line of sight (LOS) points directly into the anti-sun direction to get the maximum phase angle for possible targets. Sun-synchronous orbits (SSO), especially the dawn/dusk type of SSO have an advantage of a stable geometry according to the Sun direction during the year, which allows performing observations in the anti-sun direction without being interrupted by the Earth in the FOV. For our space-based simulations such a dawn/dusk SSO orbit was chosen.

4. INPUT PARAMETERS

Due to the fact, that we assumed two different observations scenarios, ground- and space-based, we chose different telescopes and sensors parameters for each of these scenarios. These are summarized in Tab. 1. For the ground-based sensor (GBS) we chose a large telescope, as well as a large sensor. A telescope with 1.0-meter aperture and sensors dimensions from 4,200 x 4,200 pixels to 16,800 x 16,800 pixels was simulated. For SBS, due to the technical difficulties, as well financial constrains, a telescope with an aperture of 0.3-meter was chosen with sensors dimensions varying from 2,000 x 2,000 pixels to 6,000 x 6,000 pixels. The pixel size was slightly different for both scenarios, with 15.0 µm for the ground-based and with 16.5 µm for the space-based case.

Sensor parameter	Ground-based surveillance	Space-based survey
Aperture [m]	1.0	0.3
Field of View [deg x deg]	7 x 7	5 x 5
Pixel size [μm]	15.0	16.5
Pixels per row/column [pix] **Pixel scale [arc-sec/pix]**	16,800 x 16,800 1.5	6,000 x 6,000 3.0
Pixels per row/column [pix] **Pixel scale [arc-sec/pix]**	8,400 x 8,400 3.0	4,000 x 4,000 4.5
Pixels per row/column [pix] **Pixel scale [arc-sec/pix]**	4,200 x 4,200 6.0	2,000 x 2,000 9.0

Tab. 1. Space- and ground-based telescopes and sensors parameters assumed during simulations

However, except the sensors parameters, there were also other settings which had to be set up. For every observation scenario it is necessary to know what would be the frame-rate, the astrometric accuracy, and the epoch registration accuracy. These values used during the simulations are listed in Tab. 2. The number of pixels per sensor and size of FOV are defining the pixel scale. In general, the astrometric accuracy is a function of pixel scale, object's brightness, atmospheric conditions (seeing) (this is only relevant for ground-based sensor) and sensor's position accuracy (this is only relevant for space-based sensor). Finally, all these parameters lead to an astrometric noise included into the measurements. In our simulation we assumed for astrometric noise two different approaches. For space-based sensor the one fifth of pixel scale was assumed as an astrometic noise added to observations. For ground-based sensor, due the atmospheric effects, this value was set to one half of pixel scale. For the GBS the frame-rate values were chosen to be 2, 4, 8 and 12 frames/s and for the SBS these values were 0.333, 2, 4 and 50 frames/s. The first two values represent the capabilities of CCDs, while the other two values represent capabilities of CMOS cameras. The last parameter, which was necessary to introduce during simulations was the epoch registration accuracy. We have chosen value 0.00864 ms, which is the equivalent to the precision of the PROOF (ESA's Program for Radar and Optical Observation Forecasting [4], the software introduced in the next section) output files, hence the lowest value we could get during simulations. A value of 0.025 ms, which is theoretically the value reachable by current CMOS cameras by using electronic shutters, and values 0.5 ms and 20.0 ms, which are values reachable by the CCDs by using mechanical shutters. The same values for these parameters were chosen for the SBS. In Tab. 2 we also summarized populations used during simulations. The MASTER-2009 population [4] was used, where for the LEO we considered only objects within the size interval 1 cm - 100 m and a ranges <6,000 km and <3,500 km for the ground-based and space-based scenario, respectively. For the GEO population only objects between sizes 5 cm - 100 m and range within interval between 35,000 - 55,000 km were taken into account during both scenarios.
Within this paper the LEO objects are defined as objects with mean altitude above the Earth surface less than 2,000 km. For GEO the definition is that the orbit apogee is below 37,786 km altitude, the perigee is altitude above 33,786 km and with the orbital inclination below 20°.

Sensor parameter	Ground-based surveillance	Space-based survey
Pixel scale [arc-sec/s]	1.5 / 3.0 / 6.0	3.0 / 4.5 / 9.0
Astrometric accuracy [arc-sec]	~0.0 / 0.75 / 1.5 / 3.0	~0.0 / 0.6 / 0.9 / 1.8
Frame-rate [frames/s]	2 / 4 / 8 / 12	0.333/ 2 / 4 / 50
Epoch accuracy [ms]	0.00864 / 0.025 / 0.5 / 20.0	0.00864 / 0.025 / 0.5 / 20.0
Used population	MASTER-2009 LEO (1 cm – 100 m, range<6000 km) / GEO (5 cm – 100 m, 35000 – 55000 km)	MASTER-2009 LEO (1 cm – 100 m, range<3500 km) / GEO (5 cm – 100 m, 35000 – 55000 km)

Tab. 2. Different input parameters and settings used during space- and ground-based sensors simulations.

For the simulations the results from the astrometric analysis need to be combined with observations from simulated strategies, and subsequently an initial orbit determination can be performed. The accuracy of the determined orbit as a function of the precision of the astrometric data can be evaluated. PROOF can be used to simulate the detection of a reference population with different observation scenarios. Such simulations provide an estimation of the population coverage and, on the other hand, a realistic radiometric performance. A list of observations, generated using PROOF detection events, can be used as input for the initial orbit determination. PROOF is provided with a plug-in interface that allows outputting the observation geometry for all so-called crossing/detected objects. The orbit determination software ORBDET that is part of the CelMech program system [5] has been extended to support

the simulated observations from PROOF's plugin output. ORBDET allows adding normal-distributed noise to the observable right ascension and declination. The orbit calculated with ORBDET can be compared with the known "true" orbit and the quality of the orbit can be evaluated. During the initial orbit determination always simplified model for the perturbations was assumed including the oblatness term C_{20} and the third-body perturbations due to the Sun and Moon [5].

5. SIMULATIONS

Several simulations were performed for the ground-, as well the space-based system with always the same scenario, but different input parameters. Different values were used for astrometric accuracies, frame-rates and epoch registration accuracies (see Tab. 2).
For the ground-based surveillance scenario 1 to 3.5 minutes of observations were simulated. During this periods of time, 1 and 3.5 minutes, 1,104 and 2,551 LEO/MEO objects and 260 and 287 GEO/other objects crossed 14 simulated FOVs. The closest range between the object and the sensor was 564 km. This can be seen in Fig. 2 left, where the closest sensor-object range is plotted as a function of the object inclination. Fig. 3 left shows the angular velocity distribution of tracked objects during their closest approach. The maximum number of objects had an angular velocity between 794 - 1000 arc-sec/s (0.22 – 0.28°/s) and the fastest had values around 0.85°/s. Most of objects were observed for only one second and had only one tracklet (52.3 %). 32.6 % of the observed objects had two tracklets, 10.3 % three tracklets , and four were observed for 4.4 % of the objects.
For GEO/other population, for which the data are not plotted, the objects had angular velocities between 9 to 18 arc-sec/s, with a maximum in the interval from 12.6 – 18 arc-sec/s. Most of the GEO/other objects had 10 tracklets in total, which is the maximum number of tracklets they could reach within the 3.5 minute long simulated time (1 tracklet every 21 s, for 3.5 minutes results in 10 tracklets).
For the space-based survey scenario the duration of the survey was equal to one sensor orbital period, hence 100 minutes (1.7 hours). During this time interval almost 10,000 simulated LEO/MEO objects and 270 GEO/other objects crossed the SBS's FOV. In Fig. 2 right are plotted the inclination vs. the object-sensor range during the closest approach. Some of these objects were closer than 50 km from the sensor and the minimum range was 12 km. Fig. 3 right shows the angular velocity distribution of the tracked objects during their closest approach. The majority of objects had angular velocity between 1000 - 1585 arc-sec/s (0.28 – 0.44°/s) and one object even reached the value of 68°/s (same object which had 12 km range). These extremely high angular velocities caused that these objects were observable only for less than few tenths of a second. Nevertheless, the majority of tracklets had lengths between 5 to 15 seconds.
For GEO/other population the objects had angular velocities between 21.6 to 61.2 arc-sec/s.

We used the output from PROOF as inputs to the program ORBDET to determine initial orbits by assuming a circular orbit for most cases.

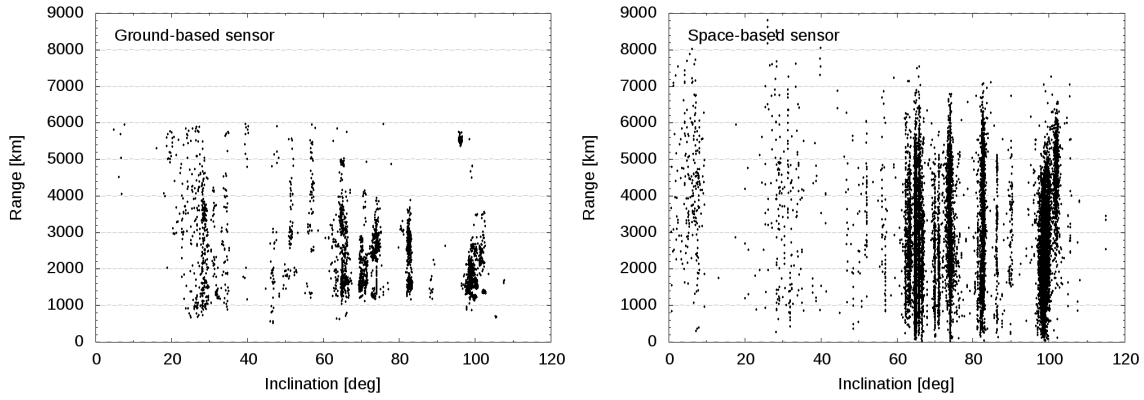

Fig. 2. Inclination vs. minimum sensor-object range for LEO objects which crossed the FOV during the simulations performed for the ground-based sensor (panel on the left) and the space-based sensor (panel on the right). There were in total 2,551 FOV-crossing objects for the ground-based (3.5 minutes of survey) and 9,500 crossings for the space-based sensor (100 minutes of survey). The statistical ESA MASTER population was used and only objects within the size range from 1 cm to 100 m were considered.

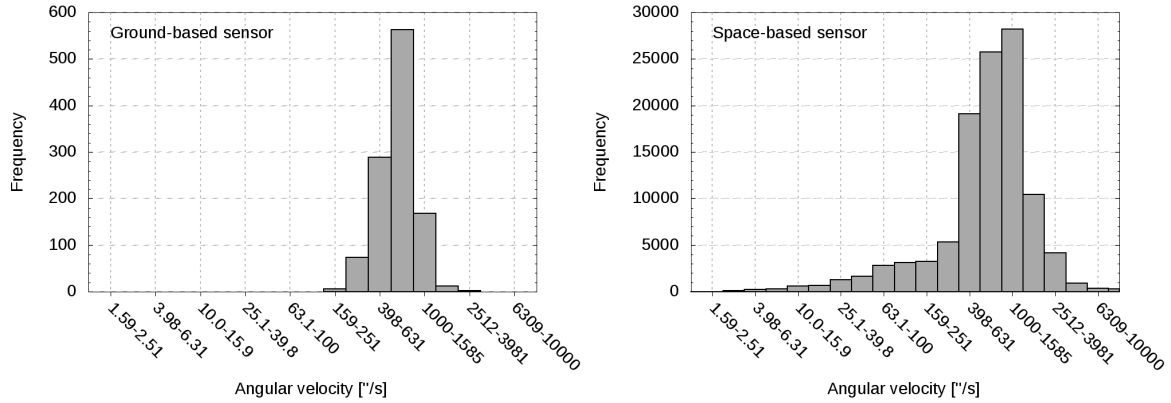

Fig. 3. Relative angular velocity for LEO objects which crossed the FOV during the simulations performed for the ground-based sensor (panel on the left) and the space-based sensor (panel on the right). There were in total 2,551 FOV-crossing objects for the ground-based and 9,500 crossings for the space-based sensor. The statistical ESA MASTER population was used and only objects within the size range from 1 cm to 100 m were considered.

For more than 99% of crossings for LEO/MEO and GEO/others from the ground-based scenario, the initial orbit was determined and compared to the true orbit. For the space-based scenario we obtained on average, depending on the simulation parameters, 70% of LEO and GEO crossings for which the initial orbit determination converged. For about 25% of the LEO cases we were able to perform an orbit improvement and determine elliptical orbits.
Once the initial orbit was available, we compared it with the true orbit. We evaluated the differences for parameters such as the determined geocentric position, and velocity, and orbital elements such as the semi-major axis and the orbital plane defined by the inclination and right ascension of ascending node (RAAN). For these output parameters we investigated how the different simulation input parameters influenced the accuracies.
Fig. 3 to Fig. 6 show results for the space-based scenario assuming different frame-rates (Fig. 3 and Fig. 4) and epoch registration accuracies (noises) (Fig. 5 and Fig. 6). For the frame-rate sensitivity we clearly see improvements for the determined inclination (Fig. 4), and slightly also for the determined semi-major axis (Fig. 3) by using higher frame-rates. Here we got worst results, as expected, for the case of 1 frame per 3 seconds, or 0.3333 frames/s (fps), which is marked as red.
Similar results we obtained for the epoch registration accuracy. For the inclination its influence is very strong. The difference between the mechanical shutter epoch registration accurracy equal to 20.0 ms (marked as red in Fig. 6) and the electronic shutter equal to 0.025 ms (marked as blue in Fig. 6) is evident. For the similar frame-rate case the semi-major axis accuracy is, however, less sensitive for this input parameter than the inclination.

6. DISCUSSION

For the space-based LEO the improvements between the highest frame-rate of 50 fps (marked as orange), which represents the CMOS detector capabilities and the lowest frame-rate of 0.3333 fps (marked as red), representing the typical CCD capabilities, range from 20 to 130 % depending on the output parameter. The lowest influence was observed for the semi-major axis, while the strongest for the position vector. An improvement of 30 % in accuracy in all investigated parameters between cases with frame-rates 2 fps and 4 fps was observed. The frame-rate also increased the accuracy for LEO objects observed with the ground-based scenario, but in this case only slightly. The improvement between the fastest frame-rate of 12 fps and slowest of 2 fps was only in order of 0.5 – 1.0 %. We did not observe any significant improvement in the accuracies of the determined initial orbits for GEO, neither for the ground-, nor the space-based scenario resulting from different frame-rate values.
Due to the highest angular velocities with respect to the sensor, LEO objects observed during the space-based scenario were most affected by changes in the epoch registration accuracy (example cases plotted in Fig. 5 and Fig. 6). The improvement between the smallest theoretical value for the electronic shutter 0.025 ms (marked as blue in Fig. 5 and Fig. 6) and the mechanical shutter value of 20.0 ms (marked as red in Fig. 5 and Fig. 6) was in order of 66 – 190 % depending on investigated parameter. The epoch noise also had an influence on LEO objects observed during the ground-based scenario. The improvement between the lowest and highest accuracy values was between 0.6 – 3.0 % for investigated parameters.

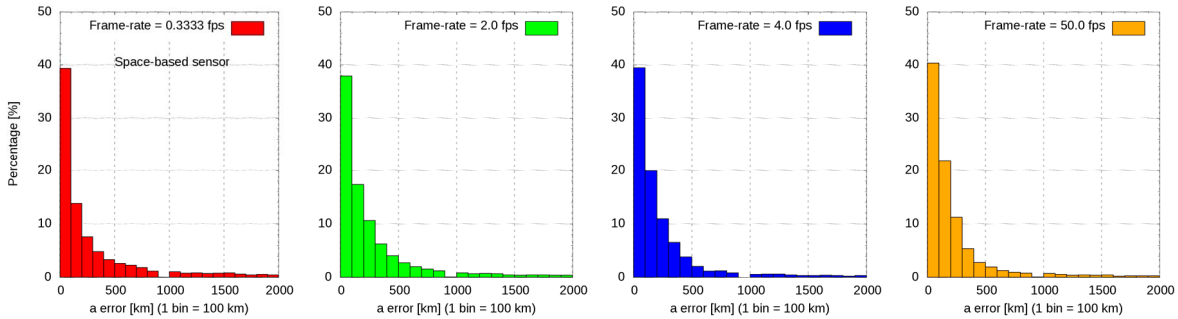

Fig. 3. An error in the determined semi-major axis [km] as a function of percentage of objects per given bin by using different frame-rate values for the space-based sensor observation scenario. There were in total 4493 LEO objects (100 % in figure) with a determined initial orbit for all four cases.

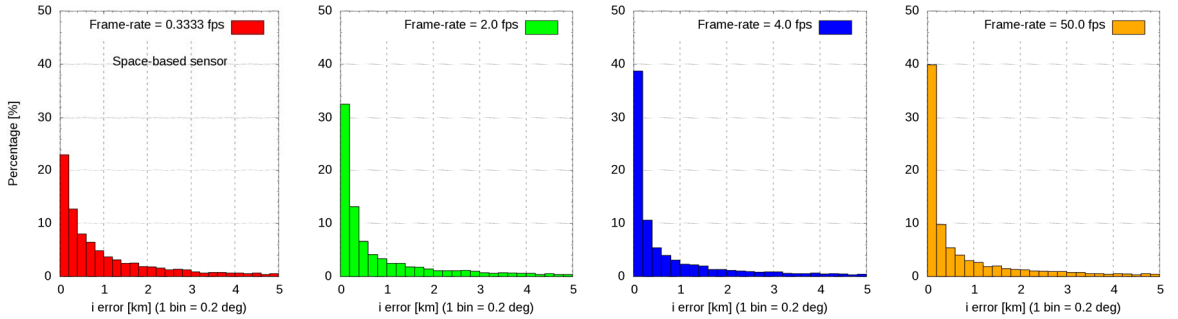

Fig. 4. An error in the determined inclination [deg] as a function of percentage of objects per given bin by using different frame-rate values for the space-based sensor observation scenario. There were in total 4493 LEO objects (100 % in figure) with a determined initial orbit for all four cases.

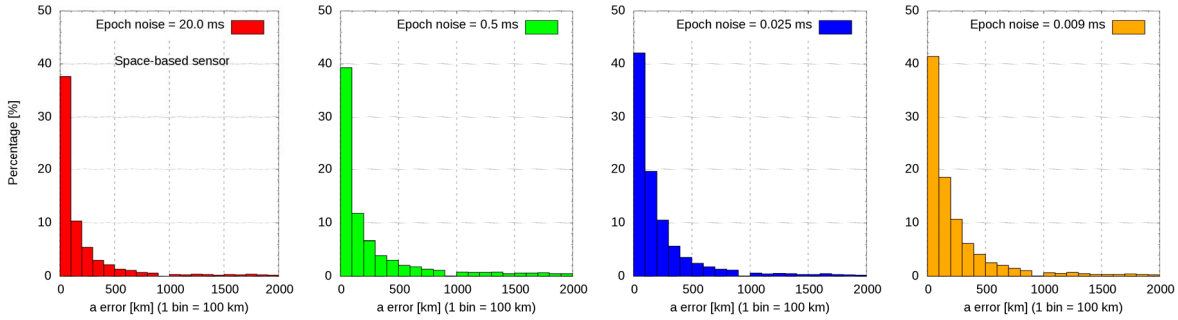

Fig. 5. An error in the determined semi-major axis [km] as a function of percentage of objects per given bin by using different epoch registration accuracies for the space-based sensor observation scenario. There were in total 6129 LEO objects (100 % in figure) with a determined initial orbit for all four cases.

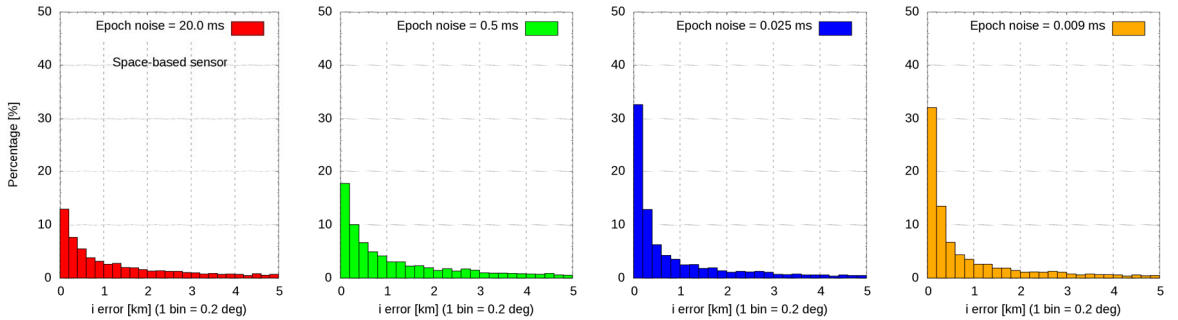

Fig. 6. An error in the determined inclination [deg] as a function of percentage of objects per given bin by using different epoch registration accuracies for the space-based sensor observation scenario. There were in total 6129 LEO objects (100 % in figure) with a determined initial orbit for all four cases.

There was no improvement observed by using higher accuracies for epoch registration for GEO objects during both scenarios.
As expected, the astrometric noise had direct influence on the accuracy of the determined initial orbits. According to performed simulations, changing of the astrometric noise had the greatest influence for GEO objects observed during the ground-based scenario. In that case improvements between the smallest noise of 0.75 arc-sec and largest noise of 3.0 arc-sec reached values between 60 – 1900 % for investigated parameters. An improvement was also visible for LEO objects, where between the smallest and the largest noise a difference of 0.5 – 4.2 % for the investigated parameters was observed. A slightly stronger influence of the astrometric noise was observed for LEO objects in the space-based scenario. Between the lowest assumed noise of 0.6 arc-sec and largest noise of 1.5 arc-sec the improvement was between 2.0 - 10.0 %. There was no significant improvement observed for GEO objects detected in the space-based scenario.

7. CONCLUSIONS

Two different observation scenarios were simulated and introduced, a ground-based survey and a space-based survey in order to investigate the sensitivity of parameters calculated during the initial orbit determination on telescope and sensor properties. These different properties arise from differences between observations performed with Charge-Coupled Device (CCD) and Complementary Metal–Oxide–Semiconductor (CMOS) sensors. Namely, we were interested if and how the astrometric accuracy, the epoch registration accuracy and the frame-rate can influence the determined orbital parameters such as the geocentric position and velocity vector, the semi-major axis, the inclination and the right ascension of ascending node for LEO and GEO objects.
There were two different populations investigated, the LEO and the GEO. The increased astrometric accuracy which was derived from the pixel scale resulted in three cases in an increased accuracy of initial orbit determination. The only exceptional case was the case of space-based observations of GEO objects, where only very marginal or no increase in accuracy was observed. Most sensitive on different sensor parameters were the orbits determined for LEO objects observed in the space-based survey, the LEO-LEO case. For these we observed a very strong sensitivity on all of the three input parameters. The strongest influence was observed for the change in the epoch registration accuracy, due to the fact that this population reached very high angular velocities during the detection. Except the fact, that the frame-rate itself can increase the number of positions per tracklet, we also observed that increasing this parameter can be very beneficial for the initial orbit determination of LEOs observed from LEO.
For the ground-based LEO case we observed an improvement in the initial orbit accuracy for all three input parameters. However, in this case the improvement of the accuracy was only considerable for the epoch registration accuracy, while for better astrometric accuracy, as well for higher frame-rate we observed only small improvements. For the ground-based GEO observations we did observe an orbit accuracy improvement only for increased astrometric accuracies, but not for higher frame-rates, nor for the increased epoch registration accuracy.
From the performed simulation we could qualify the potential improvements in the initial orbit accuracy if CMOS sensors with electronic shutters replace CCDs with mechanical shutters. Using CMOS sensors would be most beneficial in case of space-based LEO surveys, namely in the LEO-LEO configuration. A considerable amount of objects can be tracked during such a survey and very accurate orbits for the statistical analysis, but also for other purposes like the object correlation, can be obtained. Some improvement can be expected also for ground-based sensor observing LEO objects. Despite the fact that for GEO objects the improvement for the initial orbit accuracy would be only marginal, we did not investigate then next step, the effect on the orbit improvement accuracy. The same holds for the LEO objects. In a future study, we will analyze the benefits of CMOS sensors in terms of the accuracy when improving orbits of catalogued objects by means of new observations.

ACKNOWLEDGEMENTS

This work was performed in the context of the ESA project with contract no. 4000105602/12/D/SR.

REFERENCES

1. Cibin, L., Chiarini, M., Bertoli, A., Villa, F., Dimare, L., Farnocchia, D., Bernardi, F., Milani, A., Pinna, G. M., Zayer, I., Besso, P. M., Ragazzoni, R., Rossi A. 2011, *A dynamic observation concept as a key point for an enhanced SSA optical network,* Proceedings of the European Space Surveillance Conference WPP-321, 7-9 June 2011, Madrid, Spain, 2011.
2. Schildknecht, T., A. Hinze, P. Schlatter, J. Silha, J. Peltonen, T. Säntti, T. Flohrer, *Improved Space Object Observation Techniques using CMOS Detectors*, Proceedings of 6th European Conference on Space Debris, Darmstadt, Germany, 2013.
3. Milani, A., Farnocchia, D., Dimare, L., Rossi, A., Bernardi, F., *Innovative observing strategy and orbit determination for Low Earth Orbit space debris*, Planetary and Space Science, 62, 10-22 (2012).
4. Gelhaus J., Flegel S., Möckel M., Wiedemann C., Stabroth S., Oswald M., Krag H., Klinkrad H., Vörsmann P., *Validation of the ESA-MASTER-2009 space debris population*, Presented at 61st International Astronautical Congress held in Prague, Czech Republic, 2010, IAC-10.A6.2.1.
5. Beutler G., *Methods of Celestial Mechanics*, Springer Verlag, Heidelberg, 2005.